J Pharm Anal Vol 1, No 1, 39 - 45 (2011)

ORIGINAL ARTICLES

Synthesis of a new chitosan derivative and assay of *Escherichia coli* adsorption

Bing-Bing Shang[1], Jun Sha[1], Yang Liu[1], Qin Tu[1], Man-Lin Li[1], Jin-Yi Wang[1,2]*

[1] *College of Science, Northwest Agricultural & Forestry University, Yangling, Shaanxi 712100, China;*
[2] *Shaanxi Key Laboratory of Molecular Biology for Agriculture, Northwest Agricultural & Forestry University, Yangling, Shaanxi 712100, China.*

Abstract: A new chitosan derivative is prepared using chitosan. Ethyl chlorocarbonate was first introduced to the hydroxyl group of phthaloylchitosan through a nucleophilic reaction. Hydrazine was then added to recover the amino groups of chitosan and promote cross-linking. The structure of this new chitosan derivative was characterized by Fourier transform infrared (FT-IR) and proton nuclear magnetic resonance (^{1}H NMR) spectroscopy, and its physical properties were determined by X-ray diffraction (XRD), differential scanning calorimetry (DSC), and thermogravimetric analysis (TGA). The thermal and chemical stabilities of the new derivative were improved compared with those of native chitosan. Assay of *Escherichia coli* adhesion on a film based on this chitosan derivative showed good adsorption and biofilm formation.

Keywords: chitosan derivative; synthesis; bacterial adhesion; biofilm

1 Introduction

Chitosan, β-(1, 4)-linked 2-amino-2-deoxy-*D*-glucose, is derived from deacetylation of chitin. Known to be biocompatible, non-toxic, biofunctional, and biodegradable, it has been utilized in many disciplines, such as the pharmaceuticals, food, agriculture, and biotechnology industries, as well as environmental and biomedical engineering [1-3].

The chemical modification of chitosan is a common protocol for obtaining new chitosan derivatives with biofunctional properties, so that their applications may be expanded [4]. In previous reports, *N*, *N*, *N*-trimethyl chitosan [5], *N*, *O*-acetylchitosan [6], *N*-acetylated chitosan [7], and *N*-carbxymethyl chitosan [8] were synthesized to yield soluble chitosan derivatives; chitosan gel formation via a chitosan-epichlorohydrin adduct shows significant cell adhesion [9]; cross-linking chitosan with glutaraldehyde can improve the chemical and mechanical resistance of chitosan [10]; *N*-[(2-hydroxy-3-trimethylammonium) propyl] chitosan chloride has been synthesized to produce good antibacterial activities [11]. Many other studies are underway to prepare functional materials with good bioactivities or compatibilities [12,13].

The cationic nature of chitosan enables it to have efficient adsorption capacity for utilization in water treatment [14,15]. In this study, we synthesize a new chitosan derivative to which bacteria can adequately adhere. This derivative presents a potential for application in industrial and scientific research, and can be used as an efficient adsorption material that can adsorb and remove bacteria or negative colloidal particles from wastewater [15-17]. In addition, because of its ability to effectively promote biofilm (a structure formed by bacterial adhesion growth) formation, it can potentially be used in biofilm studies. In recent studies on bacterial biofilms, researchers have taken measures to treat the surface of culture vessels to promote biofilm formation. For example, the surface of a glass coverslip was modified with polyelectrolyte to enhance bacterial adhesion and biofilm growth [18]. The chitosan derivative produced in this study can easily form films on the surface of various equipments to boost biofilm growth. Nanomaterials based on biofilms are expected to be exploited and gradually used [19]; thus, the material in this study may have important production applications because it can promote biofilm growth.

The new chitosan derivative utilized in this study was obtained as follows: First, chitosan was protected by phtalic anhydride, and then ethyl chlorocarbonate was grafted onto its hydroxyl groups. It was finally deprotected by hydrazine, which also enables cross-linking with itself. The new derivative was characterized by Fourier transform infrared (FT-IR) and proton nuclear magnetic resonance (^{1}H NMR) spectroscopy, as well as X-ray diffraction (XRD), differential scanning calorimetry (DSC), and thermogravimetric analysis (TGA).

2 Materials and methods

2.1 Materials

Chitosan (degree of deacetylation $\geqslant$ 90%), phthalic

Received 12 June 2010; Accepted 13 August 2010
* Corresponding author. E-mail: jywang@nwsuaf.edu.cn (J. Wang).

anhydride, molecular sieves (4A), and calcium hydride were purchased from Sinopharm Chemical Reagent Co., Ltd. (Shanghai, China). Hydrazine (80%), ethyl chlorocarbonate, triethylamine, and *N*, *N*-dimethylformamide (DMF) were obtained from Tianjin Bodi Chemical Co., (Tianjin, China). Triethylamine was distilled from calcium hydride and stored over molecular sieves. DMF was distilled under reduced pressure from calcium hydride and stored over molecular sieves. All solvents and other chemicals were purchased from local commercial suppliers and were of analytical reagent grade, unless otherwise stated.

2.2 Synthesis of chitosan derivative

2.2.1 Synthesis of *N*-phthaloylchitosan

N-phthaloylchitosan was synthesized following a previously reported method [20,21]. Briefly, chitosan (1.0 g) and phalthic anhydride (2.75 g) reacted in 20 mL DMF for 6 h at 110 ℃ in a nitrogen atmosphere. The reaction mixture was then cooled to 65 ℃, and left overnight under the same conditions. After concentration, the reaction mixture was poured into 500 mL ice water. The precipitate was collected and washed thoroughly with methanol and then dried *in vacuo* overnight at room temperature. *N*-phthaloylchitosan (1.861 g) was obtained as a light-yellow powder (compound 1). FT-IR (KBr cm^{-1}): 3450 (OH), 1776 and 1714 (C=O of imide), 722 (aromatic ring), 1154 (C-O-C), and 1067 (C_3-OH). ^{1}H NMR (DMSO-d_6, mg/L): 1.7 (CH_3 in acetamide), 7.5 - 8.0 (aromatic ring), and 3.2 - 5.5 (pyranose ring).

2.2.2 Grafting ethyl chlorocarbonate on *N*-phthaloylchitosan

N-phthaloylchitosan (1.0 g) was dissolved in 3.28 mL DMF at 60 ℃. After 30 min of incubation, a catalytic amount of triethylamine and 3.28 mL ethyl chlorocarbonate were slowly dropped into the solution under a nitrogen atmosphere, and continuously reacted at room temperature for 2 d, with stirring. After concentration, the reaction mixture was precipitated in water. The crude product was washed several times with methanol and dried overnight *in vacuo* at room temperature (compound 2, 1.2309 g). FT-IR (KBr cm^{-1}): 3452 (OH), 1776 and 1718 (C=O in imide or $OCOOCH_2CH_3$), 1207 (C-O of $OCOOCH_2CH_3$), 722 (aromatic ring), 1153 (C-O-C), and 1067 (C_3-OH). ^{1}H NMR (DMSO-d_6, mg/L): 1.7 (CH_3 in acetamide), 1.05 (CH_3 in CH_2CH_3), 7.5 - 8.0 (aromatic ring), and 3.2 - 5.5 (pyranose ring).

2.2.3 Deprotection of grafted product and cross-linking

Compound 2 (1.0 g) was dissolved in 20 mL aqueous hydrazine (3.4 mL 80% hydrazine) at 80 ℃ in a nitrogen atmosphere [22]. After 48 h of reaction with stirring, the solution was concentrated, washed several times with water and methanol, and then dried overnight *in vacuo* (compound 3, 1.2872 g). FT-IR (KBr cm^{-1}): 3425 ($-NH_2$), 1719 ($OCONHNH/NH_2$), 1153 (C-O-C), and 1067 (C_3-OH).

2.3 Characterization

FT-IR spectra were recorded on a Nicolet NEXUS670 using the KBr method. ^{1}H NMR spectroscopy was performed on a Varian Mercury-400 spectrometer. Tetramethylsilane was used as an internal standard. Both compounds 1 and 2 were dissolved in d_6-DMSO. XRD patterns of chitosan and its derivative were recorded on an X-ray diffractometer (D/Max2550PC, Rigaku) with Cu/kα characteristic radiation at a voltage of 40 kV and a current of 50 mA. The scanning rate was 4°/min and the scanning range of 2θ was from 5° - 50° at room temperature. DSC measurements were carried out using a METTLER DSC823e calorimeter with a heating rate of 10 ℃/min. TGA was carried out using a METTLER TG/DSC1 with argon at a flow rate of 50 mL/min and a heating rate of 10 ℃/min from 25 - 700 ℃. The morphology of compound 3 films on different substrates was observed in the air after drying at room temperature with an AJ-III atomic force microscope (AFM, Nano Science Development Ltd., Shanghai, China).

2.4 Swelling test

The swelling capacity of the chitosan derivative was studied in different media. Briefly, pre-weighted derivative samples (0.05 g for each test) were separately immersed in 30 mL 0.10 M acetic acid, 0.10 M HCl, ultra pure water, and 0.10 M NaOH [23]. The samples were then retrieved from the media when they reached equilibrium swelling (24 h), wiped with filter paper, and weighted. The swelling ratio of each sample was determined according to the following equation:

$$\text{Swelling ratio}\ (\%) = \frac{(W_t - W_0)}{W_0} \times 100\%$$

where W_t and W_0 represent the weight of the swollen and dry samples, respectively.

2.5 Bacterial adhesion and biofilm formation

The bacterial species, recombinant *Escherichia coli* HB101 pGLO, was used in this study. *E. coli* HB101 was first cultured overnight at 37 ℃ on Luria-Bertani (LB) agar plates. A colony of 2 - 3 mm in diameter was then inoculated in 3 mL of LB culture medium. A total of 120 mg arabinose was added into the LB culture medium to induce the green fluorescent protein expression of *E. coli* HB101. Afterwards, the bacteria and arabinose-contained LB culture medium were diluted to 300 mL using the same medium for the next study [24].

Φ30 mm glass and polystyrene culture dishes were used to investigate bacterial adhesion and biofilm formation onto different substrates: native glass and chitosan derivative-coated glass dishes; and native polystyrene and chitosan derivative-coated polystyrene dishes.

For bacterial adhesion assay, 0.5 mL of the *E. coli* HB101 culture medium was separately incubated onto the different substrates for some time at 37 ℃. To investigate the temporal growth state of *E. coli* on different substrates, four incubation times (i.e., 12, 24, 48, and 72 h) were used for each substrate; each test was repeated at least

three times. Phase contrast and fluorescent images of *E. coli* grown on the different substrates were recorded using an inverted microscope (Olympus, CKX41) equipped with a CCD camera (QIMAGING, Micropublisher 5.0 RTV) and a mercury lamp (Olympus, U-RFLT50) after washing with sterile PBS (0.01 M, pH 7.4).

3 Results and discussion

3.1 Synthesis of the new chitosan derivative (compound 3)

Synthesis of the new chitosan derivative (compound 3) was accomplished via a three-step reaction. First, the amino groups of chitosan were protected using phthalic anhydride through a phthaloylation reaction. According to the integration of the phthaloyl protons against the protons of the glucosamine backbone, the degree of substitution was about 1.3 (Anumansirikul, 2008). Ethyl chlorocarbonate was then grafted onto the amino-protected chitosan under homogeneous conditions. Finally, hydrazine was added to deprotect the phthaloyl group. The deprotected chitosan derivative molecules cross-linked with each other to form the targeted derivative, compound 3. The complete synthetic process is shown in Figure 1.

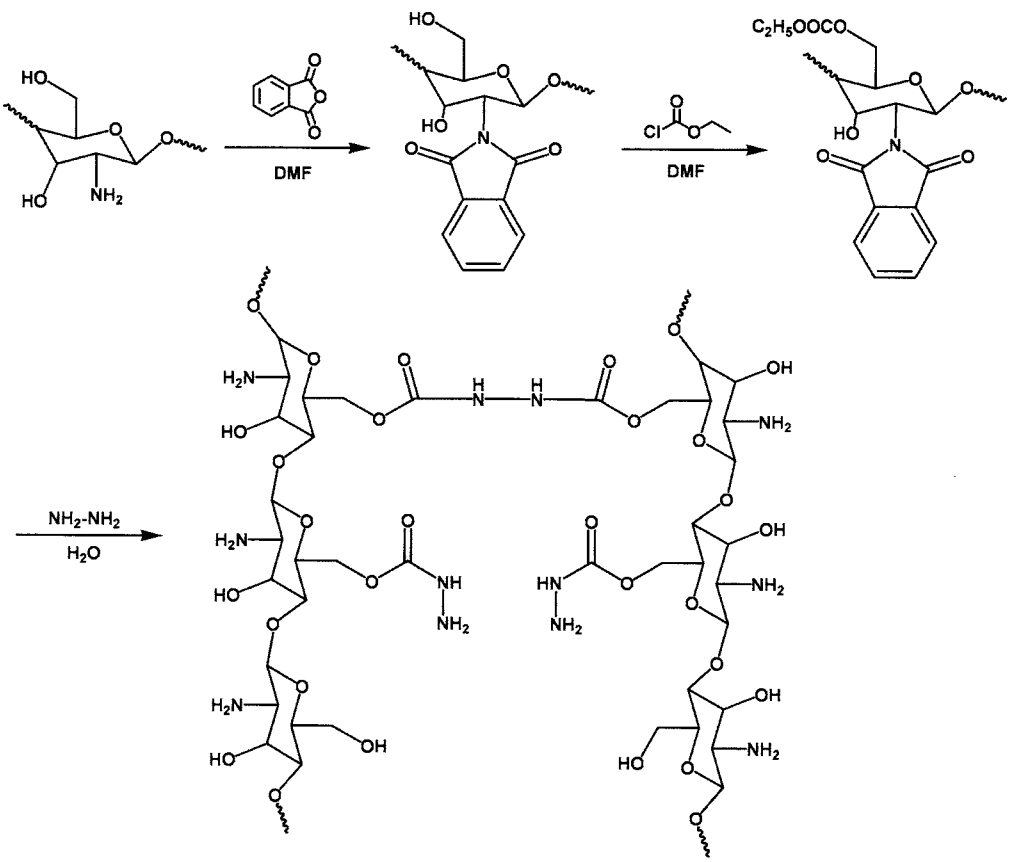

Figure 1 Complete synthetic process of the new chitosan derivative (compound 3).

Figure 2 shows the FT-IR spectra of chitosan, and compounds 1, 2, and 3. Compared with the spectra of chitosan before (a) and after (b, c, and d) protection, the peaks at 1776, 1714 (phthalimido group), and 722 cm^{-1} (aromatic ring) in spectrum (b) revealed that chitosan was successfully protected. The second step involved the grafting of ethyl chlorocarbonate to the hydroxyl groups of chitosan. The absorption band at 1391 cm^{-1} in spectrum (c) can be attributed to the $-CH_2CH_3$ characteristic vibrations of ethyl chlorocarbonate, which were stronger than those of compound 1. The band at 1718 cm^{-1} also became stronger, which can be attributed to the appearance of new -OCOO- groups. Additionally, ^1H NMR showed the methyl group of ethyl chlorocarbonate at 1.03 – 1.07. These results indicated that ethyl chlorocarbonate was successfully grafted onto chitosan. When hydrazine was added, the peaks at 1776, 1714, and 722 cm^{-1} disappeared (spectrum d), suggesting that deprotection was successful. The peak at 1709 cm^{-1} is attributed to OCO-NH-NH/NH_2 [25,26].

3.2 Physical properties of the chitosan derivative

The crystallographic structures of chitosan and its derivative were determined by XRD. Figure 3 shows that chitosan has two different peaks at $2\theta = 10^\circ$ and $2\theta = 20^\circ$. The peak at 10° was assigned to crystal form I and the strong peak at 20° was assigned to form II [27]. For the chitosan derivative, the peak at 10° was absent, and the reflection at 20° also significantly decreased. This result suggested that the crystallinity of chitosan was significantly disrupted, and the new chitosan derivative was more amorphous. This can be explained by the supposition that the cross-linked structure enables glucosamine units to become more involved inside the polysaccharide sequence to decrease the strength of the hydrogen bonds of the new compound and retard its crystallization [28].

DSC thermograms of chitosan and its derivative are shown in Figure 4(A). Chitosan showed an endothermic peak at 100 ℃ and a sharp exothermic peak at 308 ℃. The former may be due to the thermal evaporation of bound water that could not be removed completely upon drying [29], whereas the latter may be attributed to the decomposition of chitosan [30]. The chitosan derivative had no endothermic peak at 100 ℃ because of the adequate dryness of the

sample. The exothermic peak at 345 ℃ was caused by its thermal decomposition. The results indicated that the structure of chitosan chains was changed. The cross-linking process caused chitosan to form a network that improved its thermal stability.

Thermographs of chitosan and its derivative are shown in Figure 4(B). Chitosan showed slow weight loss beginning at 100 ℃ because of the decomposition of polymers with low molecular weights, followed by obvious weight loss from 259 – 310 ℃, which is attributed to the decomposition of high molecular weight groups, including the dehydration of the saccharide rings, and the depolymerization and decomposition of the acetylated and deacetylated units of the polymer [31]. The chitosan derivative showed a fast weight loss process from 269 – 325 ℃. At higher temperatures, the chitosan derivative exhibited slower weight loss than did chitosan. The results indicated that cross-linked chitosan formed a network that rendered it more thermally stable [32-34].

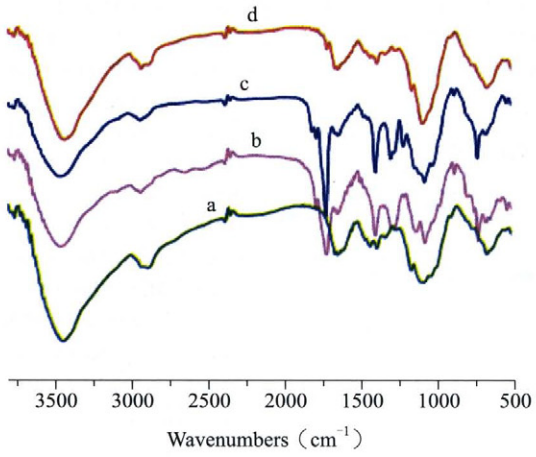

Figure 2 FT-IR spectra of chitosan(a), compound 1(b), compound 2(c), and compound 3(d).

3.3 Swelling behavior of compound 3

The swelling behavior of compound 3 was investigated using four solvents — acetic acid , hydrochloric acid , water , and sodium hydroxide. The equilibrium swelling ratio of compound 3 in ultrapure water (89.3%) was the smallest of the four solvents (acetic acid, 323%; hydrochloric acid, 294%; and sodium hydroxide, 201%). However, the swelling ratios of compound 3 in acidic and alkaline media were higher than that in water. A possible reason for this is that the cross-linked structure, which has many electric charges, can interact with dielectric media. Compared with the alkaline medium, NaOH, the swelling ratio of compound 3 in acidic medium was slightly higher, which can be explained by the assumption that in acidic medium, the amino groups of the chitosan derivative can be protonated. Hence, electrostatic repulsive forces between the charged sites cause increases in swelling. At higher pH, the charge is neutralized, causing the chain to lose repulsion and leading to shrinking [35]. Chitosan can dissolve in acetic acid because the protonation of primary amino groups causes chains of chitosan to fall apart [36]. After the cross-linking treatment in this study, however, network formation was found to improve the chemical stability of the chitosan derivative so that it exhibited good swelling behavior in acetic acid.

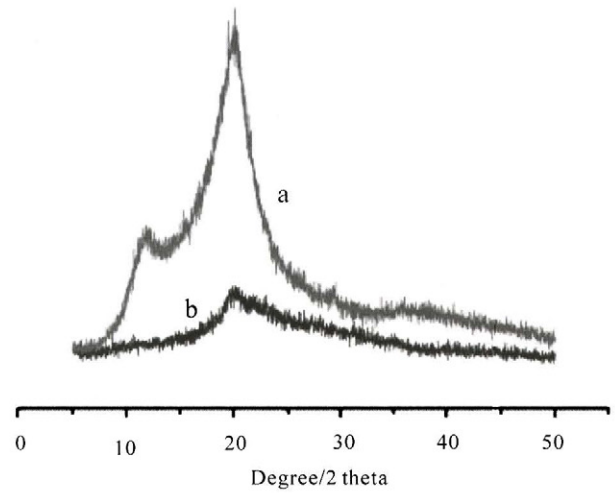

Figure 3 X-ray diffractograms of chitosan (a) and compound 3(b).

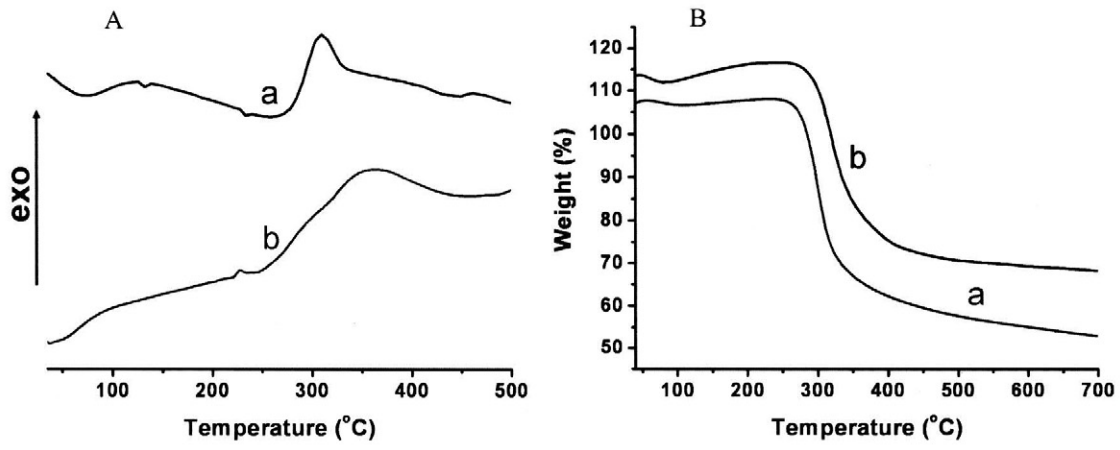

Figure 4 DSC thermograms (A) of chitosan(a) and compound 3(b), and thermogravimetric curves(B) of chitosan(a) and compound 3(b).

3.4 Morphology of compound 3 film

To investigate bacterial adsorption on the film of compound 3, the morphology of compound 3 film coated on a glass dish was observed as an example, under an inverted phase contrast microscope and AFM. Figure 5 shows the surface optical and AFM images, which illustrates that the surface of the compound 3 film was uneven or rough. This phenomenon can be utilized to explain why this derivative can adsorb bacteria and even enhance biofilm formation [37].

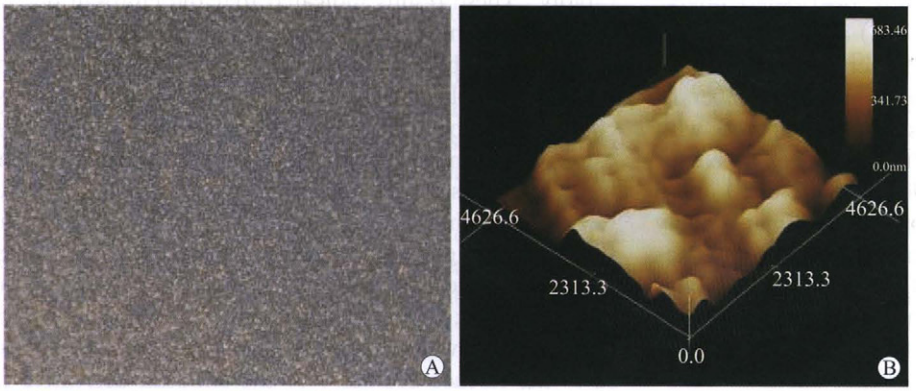

Figure 5 Optical (A) and AFM images (B) of the compound 3 film on a glass surface.

3.5 Bacterial adhesion

We chose recombinant *E. coli* HB101 pGLO for bacterial adhesion studies. This strain contains exogenous genes and can express green fluorescent proteins. As a commonly used analytical method, the fluorescent intensity of bacteria was used to represent bacterial amounts [38].

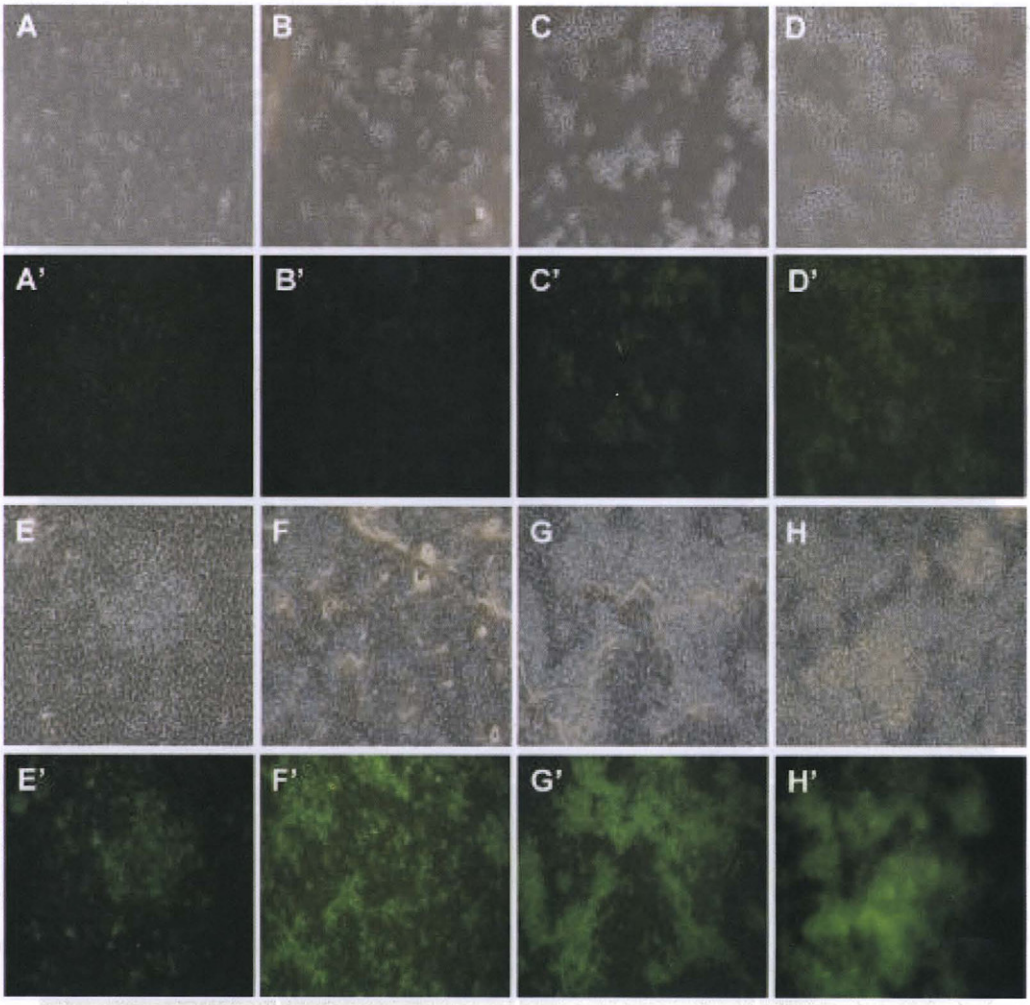

Figure 6 Optical (A－D, E－H) and corresponding fluorescence micrograph images (A'－D', E'－H') of bacterial adhesion on native glass surfaces cultured for 12 (A and A'), 24 (B and B'), 48 (C and C') and 72 h (D and D'), and on compound 3-coated glass surfaces cultured for 12 (E and E'), 24 (F and F'), 48 (G and G'), and 72 h (H and H').

Figure 6 shows the images of bacterial adhesion on bare glass (control group) and compound 3-coated glass (experimental group) at 12, 24, 48, and 72 h. As shown in Figure 6(A') and 6(B'), weak fluorescence exhibited few bacteria on bare glass; from the optical images of Figure 6(A) and 6 (B), we can see that the bacteria were distributed singly, and no biofilm appeared. In Figure 6(E') and 6(F'), strong fluorescence was observed and the bacteria formed a biofilm, which implies that a significantly larger number of bacteria adhered onto the coated surface compared with bare glass. In the control groups, after 48 and 72 h, bacterial number increased but remained low [Figure 6(C) and 6 (D)]; small stocks of the biofilm appeared but many singly distributed bacteria existed all the same, indicating low bacterial adhesion. By contrast, in the experiment groups [Figure 6(G) and 6(H)], bacterial number significantly increased and large stocks of biofilm were formed on the modified glass. These results indicated that bacterial adhesion was more appreciable on the modified surface than on bare glass.

Figure 7 shows images of bacterial adhesion on a polystyrene surface and a compound 3-coated polystyrene surface at 12, 24, 48, and 72 h. The results were similar to those of the glass groups. Bacterial adhesion in the experiment groups was more significant than that in the control groups.

Comparing the graphs of the experimental and control groups in terms of time, it can be seen that both groups adsorbed larger number of bacteria with increasing time, although the bacterial number in the control group slowly increased, whereas that in the experimental group increased rapidly. These results indicated that the chitosan derivative has an excellent capability of adhering bacteria and forming biofilm. No obvious differences were observed between the glass and polystyrene surfaces. The amino groups of chitosan can be protonated in solution. Such protonation causes chitosan to become positively charged and, therefore, highly useful in adhering negatively charged bacteria. Generally, adhesion efficiency is proportional to its charge [39]; thus, highly deacetylated chitosan has high adhesion capability. The chitosan derivative in this study has many amino groups; hence, more bacteria can adhere to it. Additionally, we speculate that adhesion capability is related to the surface geometry of the chitosan derivative film. The AFM image shows that the film formed is extremely uneven and has many microscale holes, similar to the size of bacteria. These may enable bacteria to easily sink into the small pores and adhere to chitosan [37]. This may also explain why the chitosan derivative formed a biofilm more easily than did the smooth surfaces of polystyrene and glass.

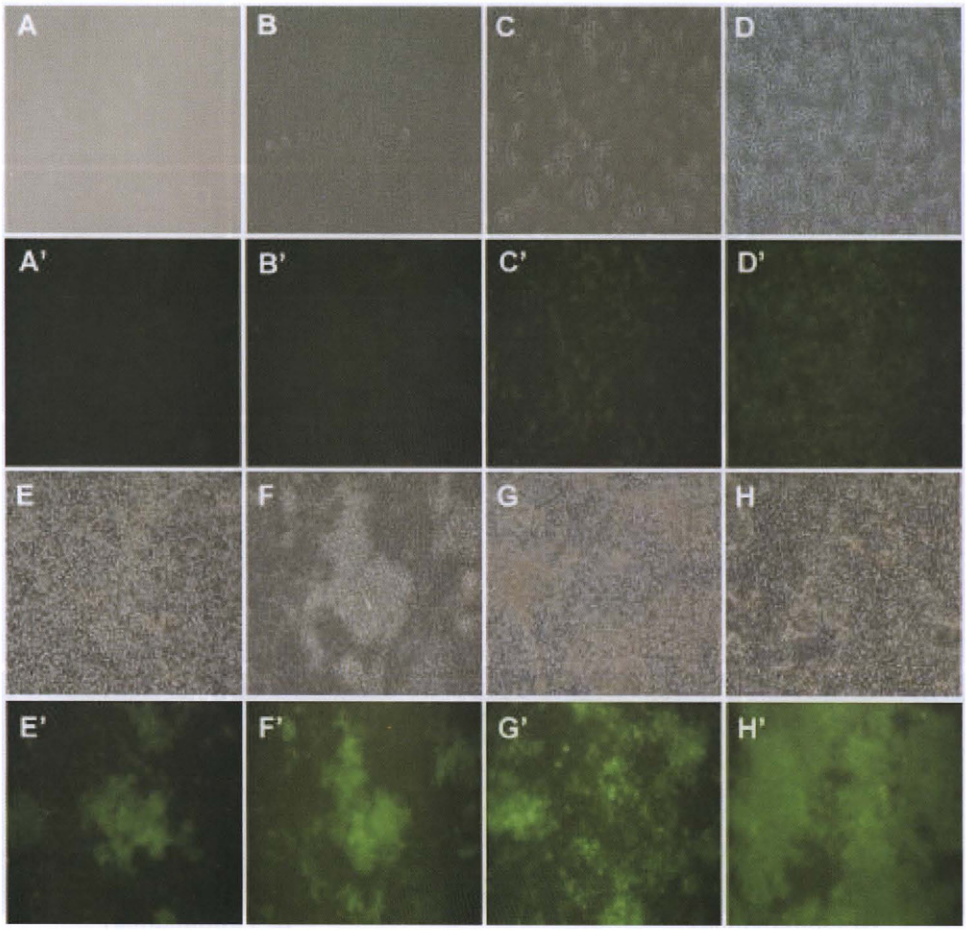

Figure 7 Optical (A – D, E – H) and corresponding fluorescence micrograph images (A' – D', E' – H') of bacterial adhesion on native polystyrene surfaces cultured for 12 (A and A'), 24 (B and B'), 48 (C and C'), and 72 h (D and D'), and on compound 3-coated polystyrene surfaces cultured for 12 (E and E'), 24 (F and F'), 48 (G and G'), and 72 h (H and H').

4 Conclusion

This study presented a new derivative by grafting ethyl chlorocarbonate onto the hydroxyl group of chitosan and cross-linked using hydrazine. The new chitosan derivative formed a network that exhibited decreased crystal properties and improved thermal stability. However, amino groups remained in the new derivative. These groups may be protonated to exist in the form of positively charged NH_3^+ groups that can attract negatively charged bacteria. The results indicate that the new chitosan derivative can enhance bacterial adhesion and biofilm formation. The derivative may also be used for future applications in bacterial adsorption in wastewater treatment and biofilm studies.

Acknowledgments

This work was supported by the National Natural Science Foundation of China (Nos. 20975082 and 20775059), the Ministry of Education of the People's Republic of China (No. NCET-08-0464), the State Forestry Administration of the People's Republic of China (No. 200904004), the Scientific Research Foundation for the Returned Overseas Chinese Scholars of the Ministry of Education, and Northwest Agricultural & Forestry University.

References

[1] Kumar MNVR. A review of chitin and chitosan applications. *React Funct Polym*, 2000, 46(1):1-27.
[2] Zhang C, Ping QE, Zhang HJ, *et al*. Synthesis and characterization of water soluble O-succinyl chitosan. *Eur Polym J*, 2003, 39(8):1629-1634.
[3] Vasudev SC, Chandy T, Sharma CP. Development of chitosan/polyethylene vinyl acetate co-matrix:Controlled release of aspirin-heparin for preventing cardiovascular thrombosis. *Biomaterials*, 1997, 18(5):375-381.
[4] Lebouc F, Dez I, Desbrieres J, *et al*. Different ways for grafting ester derivatives of poly (ethylene glycol) onto chitosan:Related characteristics and potential properties. *Polymer*, 2005, 46(3):639-651.
[5] Muzzarelli R, Baldassarre V, Conti F, *et al*. Biological-active of chitosan ultrastructural study. *Biomaterials*, 1988, 9(3):247-252.
[6] Sashiwa H, Kawasaki N, Nakayama A, *et al*. Chemical modification of chitosan. 14: Synthesis of water-soluble chitosan derivatives by simple acetylation. *Biomacromolecules*, 2002, 3(5):1126-1128.
[7] Lu SJ, Song XF, Cao DY, *et al*. Preparation of water-soluble chitosan. *J Appl Polym Sci*, 2004, 91(6):3497-3503.
[8] Muzzarelli R, Ilarl P, Petrarulo M. Solubility and structure of N-carboxymethylchitosan. *Int J Biol Macromol*, 1994, 16(4):177-180.
[9] Fangkangwanwong J, Yoksan R, Chirachanchai S. Chitosan gel formation via the chitosan-epichlorohydrin adduct and its subsequent mineralization with hydroxyapatite. *Polymer*, 2006, 47(18):6438-6445.
[10] Vieira RS, Beppu MM. Mercury ion recovery using natural and crosslinked chitosan membranes. *Adsorption*, 2005, 11:731-736.
[11] Lim SH, Hudson SM. Synthesis and antimicrobial activity of a water-soluble chitosan derivative with a fiber-reactive group. *Carbohydr Res*, 2004, 339(2):313-319.
[12] Mourya VK, Inamdar NN. Chitosan-modifications and applications: Opportunities galore. *React Funct Polym*, 2008, 68(6):1013-1051.
[13] Strand SP, Vandvik MS, Varum KM, *et al*. Screening of chitosans and conditions for bacterial flocculation. *Biomacromolecules*, 2001, 2(1):126-133.
[14] No HK, Meyers SP. Application of chitosan for treatment of wastewaters. *Rev Environ Contam Toxicol*, 2000, 163(1):1-27.
[15] Wolfaardtgm GM, Lawrence JR, Robarts RD, *et al* . Multicellular organization in a degradative biofilm community. *Appl Environ Microbiol*, 1994, 60(2):434-446.
[16] Strand SP, Nordengen T, Ostgaard K. Efficiency of chitosans applied for flocculation of different bacteria. *Water Res*, 2000, 36(19):4745-4752.
[17] Roussy J, Van Vooren M, Guibal E. Chitosan for the coagulation and flocculation of mineral colloids. *J Dispersion Sci Technol*, 2004, 25(5):663-677.
[18] Eun YJ, Weibel DB. Fabrication of microbial biofilm arrays by geometric control of cell adhesion. *Langmuir*, 2009, 25(8):4643-4654.
[19] Wang XL, Zhu H, Yang F, *et al*. Biofilm-engineered nanostructures. *Adv Mater*, 2009, 21(27):2815-2819.
[20] Rout DK, Pulapura SK, Gross RA. Liquid-crystalline characteristics of site—selectively modified chitosan. *Macromolecules*, 1993, 26: 5999-6006.
[21] Feng H, Dong CM. Synthesis and characterization of phthaloyl-chitosan-g-poly(L-lactide) using an organic catalyst. *Carbohydr Polym*, 2007, 70:258-264.
[22] Kurita K, Ikeda H, Shimojoh M, *et al*. N-phthaloylated chitosan as an essential precursor for controlled chemical modifications of chitosan: Synthesis and evaluation. *Polym J*, 2007, 39:945-952.
[23] Ngah WSW, Fatinathan S. Chitosan flakes and chitosan-GLA beads for adsorption of p-nitrophenol in aqueous solution. *Colloids Surf A: Physicochem Eng Aspects*, 2006, 277(1-3):214-222.
[24] Sambrook J, David W. *Molecular Cloning a laboratory manual*. Pei-Tang Huang translated. Third Edition. Science Press, Beijing, China, 2002.
[25] Kurita K, Ikeda H, Yoshida Y, *et al*. Chemoselective protection of the amino groups of chitosan by controlled phthaloylation:Facile preparation of a precursor useful for chemical modifications. *Biomacromolecules*, 2002, 3(1):1-4.
[26] Yoksan R, Akashi M, Biramontri S, *et al*. Hydrophobic chain conjugation at hydroxyl group onto gamma-ray irradiated chitosan. *Biomacromolecules*, 2001, 2(3):1038-1044.
[27] Samuels RJ. Solid state characterization of the structure of chitosan films. *J Polym Sci Polym Phys Ed*, 1981, 19:1081-1105.
[28] Xiao Y, Zhou XH. Synthesis and properties of a novel cross-linked chitosan resin modified by L-lysine. *React Funct Polym*, 2008, 68(8):1281-1289.
[29] Luckachan GE, Pillai CKS. Chitosan/oligo L-lactide graft copolymers: Effect of hydrophobic side chains on the physico-chemical properties and biodegradability. *Carbohydr Polym*, 2006, 64(2):254-266.
[30] Qin C, Du Y, Zong L, *et al*. Effect of hemicellulase on the molecular weight and structure of chitosan. *Polym Degrad Stab*, 2003, 80(3):435-441.
[31] Penichecovas C, Argguellesmonal W, Sanroman J. A kinetic-study of the thermal-degradation of chitosan and a mercaptan derivative of chitosan. *Polym Degrad Stab*, 1993, 39:21-28.
[32] Monier M, Wei Y, Sarhan AA, *et al*. Synthesis and characterization of photo-crosslinkable hydrogel membranes based on modified chitosan. *Polymer*, 2010, 51(5):1002-1009.
[33] Kandile NG, Mohamed MI, Zaky HT, *et al*. Synthesis and properties of chitosan hydrogels modified with heterocycles. *Carbohydr Polym*, 2009, 75(4):580-585.
[34] Li QZ, Yang DZ, Ma GP, *et al*. Synthesis and characterization of chitosan-based hydrogels. *Int J Biol Marcromol*, 2009, 44(2):121-127.
[35] Wang ZP, Feng ZQ, Gao CY. Stepwise assembly of the same polyelectrolytes using host-guest interaction to obtain microcapsules with multiresponsive properties. *Chem Mater*, 2008, 20(13):4194-4199.
[36] Rinaudo M. Chitin and chitosan:Properties and applications. *Prog Polym Sci*, 2006, 31(7):603-632.
[37] Gottenbos B, van der Mei HC, Busscher HJ. Models for studying initial adhesion and surface growth in biofilm formation on surfaces. *Biofilms*, 1999, 310:23-534.
[38] Englert DL, Manson MD, Jayaraman A. Flow-based microfluidic device for quantifying bacterial chemotaxis in stable, competing gradients. *Appl Environ Microbiol*, 2009, 75(13):557-4564.
[39] Ashmore M, Hearn J. Flocculation of model latex particles by chitosans of varying degrees of acetylation. *Langmuir*, 2000, 16(11):4906-4911.